SECTION 4
CASE STUDY OF POTENTIAL INTERFERENCE USING ADOPTED BPL RULES

4.1 INTRODUCTION

To examine the potential effectiveness of the rules for Access BPL, a case study was undertaken. The study modeled a residential neighborhood in which BPL devices had been installed on overhead power lines, with the radiation level from the BPL energized power line designed to meet FCC Part 15 rules and measurement guidelines adopted for Access BPL systems. Using this model, the potential noise floor increase seen by land mobile devices on roads adjacent to the line was determined. PFD levels resulting from BPL emissions that might be experienced at distant fixed receivers, such as for OTH radars, were also evaluated in this case study.

The modeling effort detailed herein is not intended to be representative of a typical residential neighborhood; however, the power line and nearby roads are modeled using an actual residential area in which BPL devices have been installed, and this study is therefore instructive regarding conditions that might be encountered by nearby land mobile receivers and by distant receivers under the adopted rules. It is an extension of NTIA's previous work that attempted to characterize typical interference potential due to BPL signals injected into a generic power line layout.

4.2 METHODOLOGY

The Commission's BPL Report and Order specified measurement guidelines to enable BPL providers to determine compliance of their systems with FCC Part 15 limits. The relevant measurement guidelines are as follows:

- For systems using data burst rates of at least 20 bursts per second, quasi-peak measurements are to be employed;
- For frequencies above 30 MHz, electric field sensing antennas are to be used, with the measurement height from 1 to 4 meters to maximize the measured field at the Part 15 reference distance of 10 meters. Alternatively, the measurement may be made at 1 meter height, with a correction factor of 5 dB added to the measured field;
- For frequencies below 30 MHz, a magnetic field sensing loop is to be employed at a measurement height of 1 meter, with the loop rotated about the vertical axis to maximize the measured field at the Part 15 reference distance of 30 meters;
- Measurements should normally be performed at a horizontal separation distance of 10 meters from the overhead line;

- For field strength measurements, the slant range distance between the overhead wiring carrying the BPL signals and the measurement antenna is used to compute a distance correction factor for adjusting the field strength measurement;
- For signals with a bandwidth that is less than the midband frequency, measurement points are to be at the device and at ¼-wavelength multiples of the midband frequency wavelength down the line, to a distance equal to one wavelength of the midband frequency;
- For signals with a bandwidth exceeding the midband frequency, measurement distance down the line are to be extended in ½-wavelength of the midband frequency increments until the distance equals or exceeds ½ wavelength of the lowest in-band frequency.

A computer model was constructed based upon an actual power line structure where NTIA conducted measurements of BPL emissions. The model was created with the help of *in-situ* observations and measurements, and was designed for simulation using NEC-4.1. As closely as possible and within program constraints, this model was designed to conform to the actual features of the power grid, including the use of catenary wires, correct placement of transformers loads, wire height and placement on power poles, grounding wires, riser, pole placement and wire junctions. The overall extent of the model was approximately 328 meters in the x-axis direction, and 435 meters in the y-axis direction. The modeled power line height was 12 meters. All wires were 12.6 millimeters in diameter and given the conductivity of copper (5.8×10^7 S/m). The ground plane for the model (a flat earth structure beneath the wires) had characteristics typical of "good" ground (dielectric constant of 15.0, conductivity of 0.005 S/m). Due to the computational complexity of this model, the simulations were constrained to frequencies below 30 MHz.

Simulations were focused on wideband and narrowband cases, based upon the FCC testing methodology stipulated above. For the wideband case, the BPL signal was assumed to cover the frequency range of 4 to 22 MHz, with a midband frequency of 13 MHz. For the narrowband case, signals were assumed to occupy 4 MHz bandwidth, with midband frequencies ranging from 4 MHz to 28 MHz, in 4 MHz increments.

4.2.1 Structure Injection Points

NTIA's elaborate overhead power line model has enough topological power-line features and sufficient geographic extent that simulations can be run for BPL devices placed at several points on the model. In this effort, three points in the power line structure were selected, as shown in Figure 4-1.

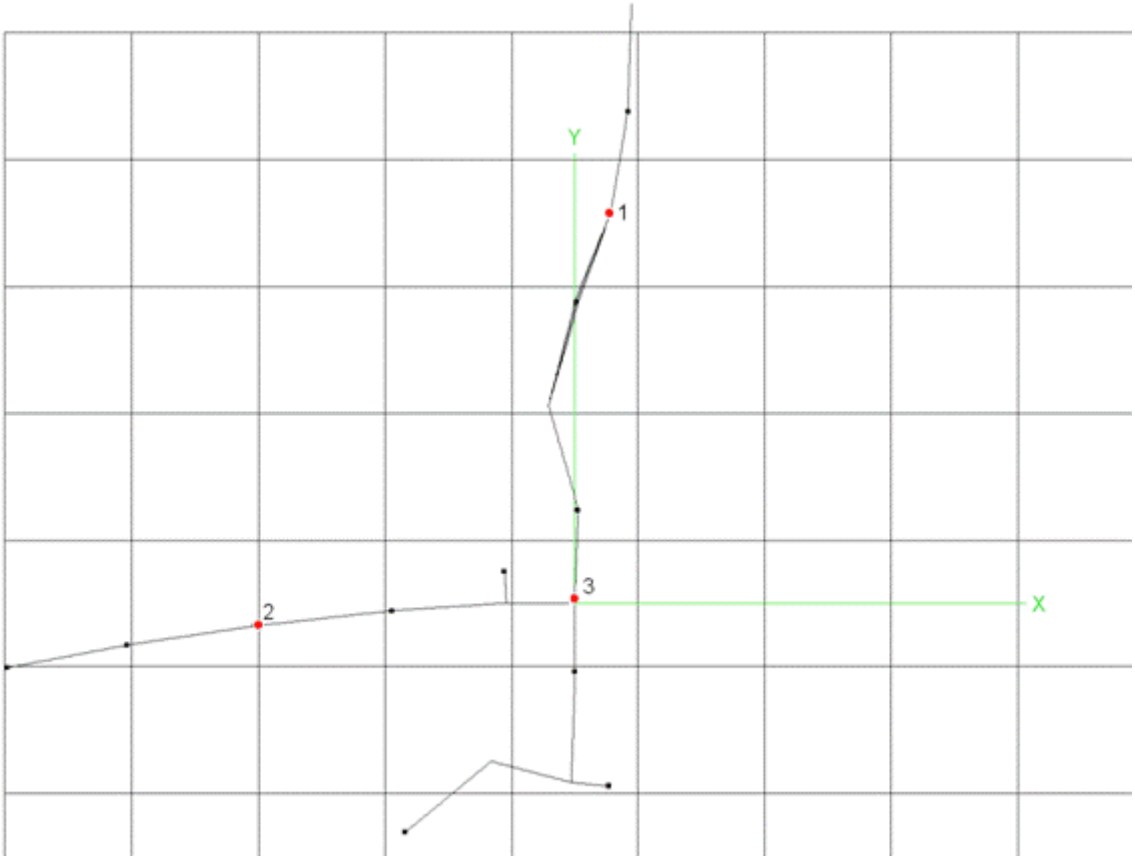

Figure 4-1: Overhead view of the power line model depicting BPL injection points (red dots). Distribution transformers (impedance loads to neutral) are shown by black dots.

In selecting the three points to be used, particular attention was paid to the magnitude and geographic extent of the radiated field around the power line structure by initial, wide-area NEC simulations of the magnetic field, as illustrated in Figure 4-2. In part, it may be assumed that the level of such radiation is influenced by the number and type of discontinuities (impedance and topological changes) encountered near each point. This methodology was used in order to better simulate expected radiation levels over a range of operating conditions and power line configurations.

4.2.2 Simulation Frequencies

For both narrowband and wideband cases, simulations were conducted at 2 MHz intervals including the lower and upper bounds of each band. The 4 MHz narrowband signals, centered at 4, 8, 12, 16, 20, 24 and 28 MHz, were simulated at three frequency points (lower bound, midband and higher bound), while wideband signals were simulated at 10 frequency points, from 4 to 22 MHz. The frequencies and midband points are detailed in Table 4-1.

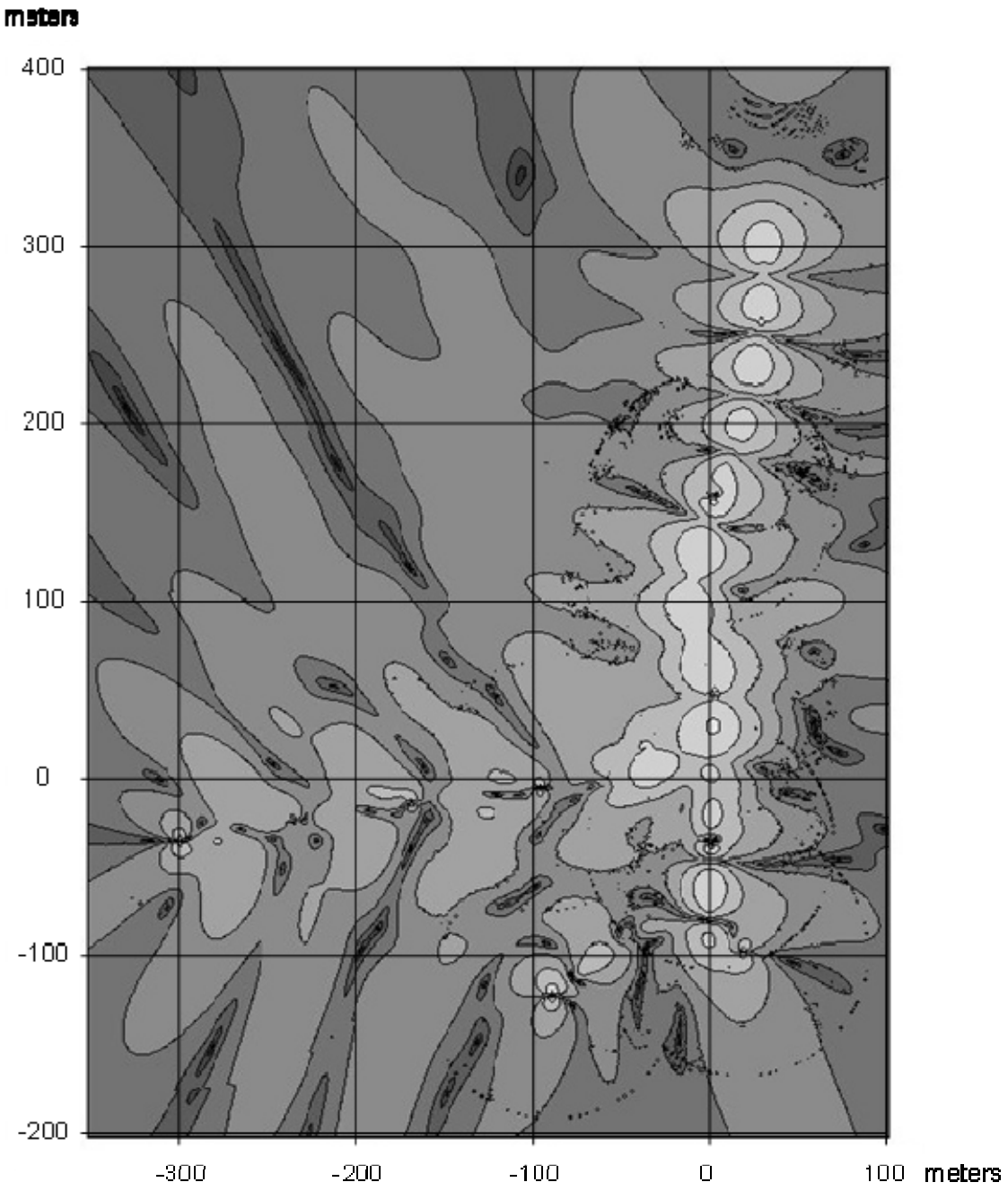

Figure 4-2: X-axis (horizontal) magnetic field due to BPL-energized power line (4 MHz), one meter off the ground, excited at point "3" and depicted in overhead view. Lighter shades represent stronger fields.

Table 4-1: NEC simulation frequencies

Frequency Band (MHz)	Midband Frequency (MHz)	Simulation Frequencies (MHz)
Narrowband Case		
2-6	4	2, 4, 6
6-10	8	6, 8, 10
10-14	12	10, 12, 14
14-18	16	14, 16, 18
18-22	20	18, 20, 22
22-26	24	22, 24, 26
26-30	28	26, 28, 30
Wideband Case		
4-22	13	4,6,8,10,12,14,16,18,20,22

4.2.3 Part 15 Scaling

4.2.3.1 Measurement points

As discussed previously, the rules adopted by the FCC specify measurement locations along the power line under two broad conditions: narrowband signals and wideband signals. For the narrowband case, measurement points are defined at the BPL energizing device, and ¼, ½, ¾, and 1 wavelength of the midband frequency away from the device down the power line. For the wideband case, the measurements are to continue down the power line at midband ½ wavelength intervals, until the total measurement distance exceeds ½ wavelength at the lowest frequency.

Lines parallel to and 10 meters away from, the power line segments were derived from the model layout, and measurement points along those lines were identified. For the wideband case, 4 MHz was assumed to be the lowest operating frequency (corresponding to a wavelength of 74.95 meters), with a midband frequency of 13 MHz (23.06 meter wavelength). As Table 4-2 illustrates, the measurement regime indicates measurements in this case should be made at points out to 2 wavelengths distant at the midband frequency from the BPL device.

Table 4-2: Distances down the line from BPL device for wideband-case Part 15 measurement points

Wavelength from BPL Device	0	1/4	1/2	3/4	1	1 1/2	2
Distance Down Power Line (m)	0	5.765	11.531	17.296	23.06	34.592	46.123

For the narrowband case, simulations were run at locations along the power line appropriate for each band's midband frequency (Table 4-3).

Table 4-3: Distances down the line from BPL device for Part 15 measurement points in narrowband case, by frequency

Narrowband Center Frequency (MHz)	Distance Down Power Line, by Wavelength (m)				
	0	**1/4**	**1/2**	**3/4**	**1**
4	0.000	18.738	37.475	56.213	74.950
8	0.000	9.369	18.738	28.106	37.475
12	0.000	6.246	12.492	18.738	24.983
16	0.000	4.684	9.369	14.053	18.738
20	0.000	3.748	7.495	11.243	14.990
24	0.000	3.123	6.246	9.369	12.492
28	0.000	2.677	5.354	8.030	10.707

Coordinates for points along the power line, 10 meters distant from the line (as specified in the BPL Report and Order, Appendix C) were calculated at the distances from the BPL injection device as specified above. Exceptions to this scheme were points at which a power line "T" branch or end caused a calculated point to be closer or farther than 10 meters from the power line. When these points were encountered, simulation results were not used.

4.2.3.2 Scaling output power to meet FCC Part 15 limits

Initial NEC simulations were used to determine the power output of each modeled BPL device that would meet Part 15 limits using the adopted BPL measurement guidelines. For the frequencies considered in this analysis (all below 30 MHz), the FCC Part 15 radiated emissions limit, E_{30m}, is specified as 30 μV/m at 30 meters horizontal distance.[53] To adjust electric field strength levels computed at the 10 meter distance specified in the Access BPL measurement guidelines, the slant range between the power line and measurement point must be used in conjunction with a 40 log correction factor. With the modeled power line height of 12 meters and measurement point height of one meter, the slant range adjustment results in an extrapolated limit at 10 meters as shown below using Equations 2-2 and 2-3.

$$E_{10m} = E_{30m} \cdot 10^{\frac{40 \cdot \log_{10}\left(\frac{30\,m}{\sqrt{(12\,m-1\,m)^2+10\,m^2}}\right)}{20}} \approx 122.2\ \mu V/m$$

For all frequencies below 30 MHz, the Part 15 measurement bandwidth is specified as 9 kHz.

The BPL energized power line radiation was simulated for the wideband case at the specified frequencies within the band (*See* Table 4-1). Magnetic field values at the geographic measurement points specified in the Part 15 measurement guidelines for Access BPL systems were calculated and converted to electric field values following Equation 2-1. The maximum of these electric field values calculated by NEC over all

measurement points and frequencies (E_{max}) was subsequently divided by E_{10m} to obtain a scaling factor, "A", used to scale the electric field strength data in the wideband case.

$$A = \frac{E_{max}}{E_{10m}} \qquad \text{(Equation 4-1)}$$

For the narrowband case, simulations were run for all specified frequencies within each band to determine the magnetic field values at the appropriate measurement points for each band (*See* Table 4-1). As with the wideband case, all values were converted to electric field values, and the maximum electric field value at any measurement point and frequency for each band was divided by E_{10m} to obtain the scaling factor, A, for each band.

4.2.4 Simulation of Potential Interference

After scaling the output power to meet the Part 15 limits for each frequency, bandwidth case, and BPL device location, the interference potential for each situation was simulated. Field-strength values were obtained from simulations both along and away from the modeled power line. From these results, noise floor level increases for a simulated land-mobile receiver located on a road next to the power line were calculated. Additionally, PFD calculations were carried out to determine the possible impact upon a radar receiver at a large distance from the power line.

4.2.4.1 Ambient noise levels

Noise levels calculated for this analysis were median values for the location in question over time of day and season. To simulate the local (*i.e.*, private residence) BPL operating conditions under which land mobile receivers might encounter BPL signals, the residential manmade noise conditions shown in Table 4-4 were used. As in the NTIA's Phase 1 Study, ambient noise was calculated using the Institute for Telecommunication Sciences NOISEDAT computer program.[54] A bandwidth of 2.8 kHz was used consistent with that of a land mobile receiver.

Table 4-4: Ambient noise power, by frequency, in a 2.8 kHz bandwidth

Frequency (MHz)	Noise Power, N_{dBW} (dBW)
2	-104.28
4	-112.08
6	-116.98
8	-121.03
10	-124.13
12	-126.28
14	-128.28
16	-130.08
18	-131.63
20	-132.93
22	-134.13
24	-135.18
26	-136.13
28	-137.03
30	-137.83

4.2.4.2 Simulation of increased noise levels along an overhead power line

NTIA analyzed the noise floor increase that may be experienced by a land mobile radio operating in close proximity to a BPL-energized MV overhead power line. The analysis was undertaken to compute the percentage of points along the power line that experienced a given increase in the noise floor above the ambient level.[55] To accomplish this, NTIA ran NEC simulations to obtain electric field values around the modeled power line. The points at which the electric field was calculated were in the path of roads found along the actual power line upon which the model was based, as shown in Figure 4-3. Electric field strength values were computed at two meters off the ground to simulate the height of a vehicle-mounted land mobile radio antenna, and at one meter increments along the path. The land mobile radio system was assumed to be using a vertical whip antenna. Accordingly, only the z-axis (vertical) electric field values were used.

The path around the modeled power line along which electric field strength values were calculated varied in distance from the power line. Along one section of the modeled power line, the horizontal distance from the power line to the center of the road was approximately 3 meters, and ranged from 30 to 48 meters along another section. The path along which calculations were performed passed under a branch of the power line model at one point (Figure 4-3).

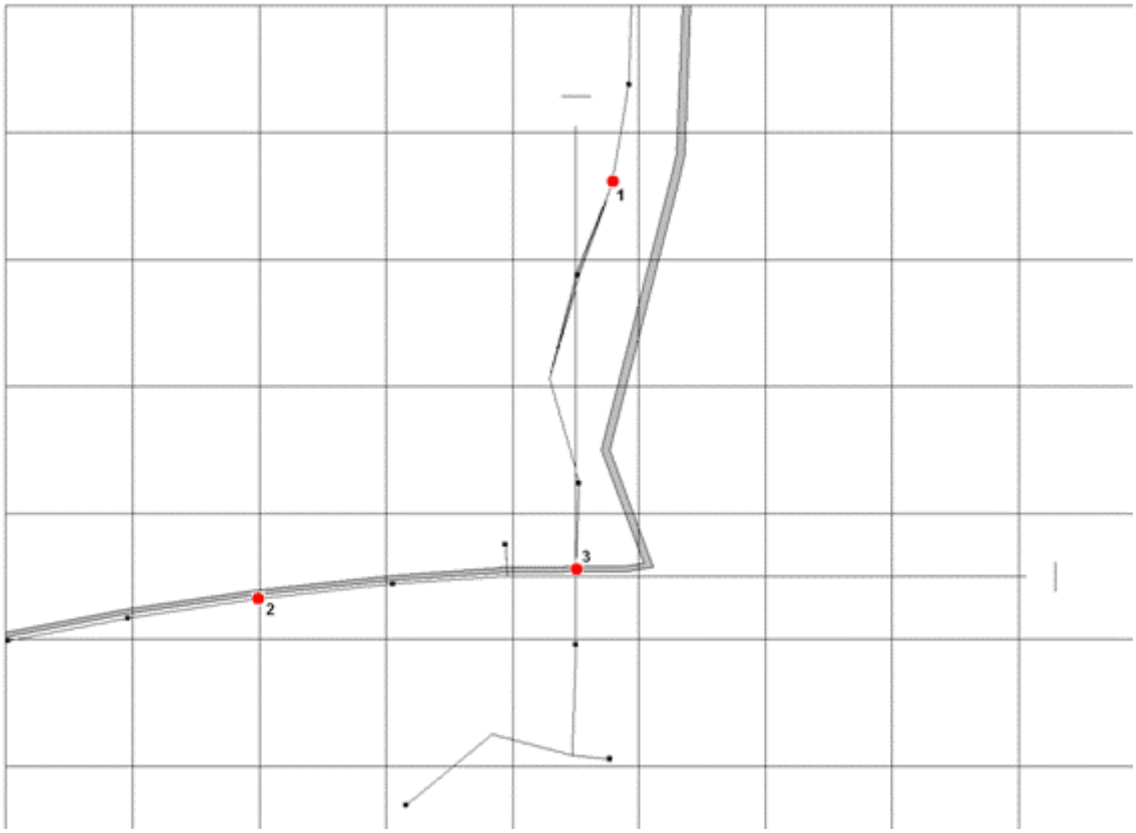

Figure 4-3: Path of along-the-line land mobile simulations (thick grey line). This path corresponds to that followed by actual road next to the power that the model is based on, depicted in overhead view.

Once derived, the electric field values were translated into received interfering signal power using Equation 4-2.

$$P = 20 \cdot Log_{10}\left(\frac{E}{A}\right) - 20 \cdot Log_{10}(F) + G_r + 10 \cdot Log_{10}(BW) + 10 \cdot Log_{10}(\phi) + \delta + 12.8 \quad \text{(Equation 4-2)}$$

where

P is received BPL signal power, in dBW;

E is the calculated vertical electric field strength, in V/m;

A is the Part 15 electric field scaling factor determined for the narrowband case, and for the wideband case, as described in Section 4.2.3.2;

F is the measurement frequency, in MHz;

G_r is the gain of the receiving antenna, in dBi;

BW is the ratio of receiver to measurement bandwidth;

ϕ is the average duty cycle; and

δ is a quasi-peak to RMS measurement factor.

As in NTIA's Phase 1 Study, the average duty cycle (ϕ) was taken to be 55 percent, which was midway between an always-on (100 percent) downstream signal and an intermittent (10 percent) upstream customer-to-internet signal. The gain (G_r) of the receiving antenna was taken to be a constant 0 dBi across all frequencies, and the ratio of receiver bandwidth to measurement bandwidth (BW) was 2.8 kHz to 9 kHz, respectively. Finally, to compensate for differences between ambient noise levels expressed in RMS values and BPL signal radiation measured using quasi-peak detection, a measurement factor (δ) adjustment of -2 dB was applied to the calculated received BPL signal power.[56]

The increase in the noise floor due to BPL emissions, or (I+N)/N, was calculated using Equation 4-3.

$$\frac{(I+N)}{N} = 10 \cdot Log_{10}\left[1 + 10^{\frac{P-N}{10}}\right] \qquad \text{(Equation 4-3)}$$

where

P is the received BPL signal power, in dB, from Equation 4-2;

N is the ambient noise power, in dB; and

I is the interfering signal, in dB.

The results of these calculations are used to determine the percentage of geographic locations that exceed given thresholds of noise floor increase.

4.2.4.3 Simulation of PFD levels away from an overhead power line

NTIA analyzed the PFD levels due to BPL emissions that may be seen by fixed receivers, such as OTH radar receivers, at increasing distances from the power line structure used in this case study. Both NEC and ITM were used to derive PFD values at 1 km intervals on radials extending out from the power line injection points. The radials were spaced 1 degree apart, for a total of 360 radials, and extended from 1 to 50 km from the origin.

Electric field strength values were calculated first using Equation 4-4 along each radial at 42.7 meters height, the height of the assumed receiver antenna. NEC calculations were performed to a distance of 10 km from the origin, a distance chosen to minimize variations due to the large size of the power line layout and diffraction effects due to the curvature of the earth. Beyond 10 km, ITM was used to calculate the basic transmission loss due to distance separation and diffraction of the RF signal over a spherical earth.

$$E_{total}(\rho) = \sqrt{E_\rho^2 + E_\phi^2 + E_z^2} \qquad \text{for } 1\,km \le \rho \le 10\,km \qquad \text{(Equation 4-4)}$$

where

E_{SUM} is electric field strength vector, in V/m;

E_z is the z-axis (vertical) component of electric field, in V/m;

E_ϕ is the phi-axis (perpendicular to radial and z-axis) component of electric field, in V/m; and

E_ρ is the rho-axis (along the radial) component of electric-field, in V/m.

The PFD was then derived from E_{SUM} using Equation 4-5.

$$PFD_{NEC}(\rho) = 10 \cdot Log_{10}\left[\frac{\left(\frac{E_{SUM}(\rho)}{A}\right)^2}{120\pi}\right] + 10 \cdot Log_{10}\left(\frac{1}{BW}\right) \quad for\ 1\ km \le \rho \le 10\ km$$

(Equation 4-5)

where

A is the Part 15 electric field scaling factor determined for the narrowband case, and for the wideband case, as described in Section 4.2.3.2;

BW is the specified Part 15 measurement bandwidth (9 kHz for signals below 30 MHz); and

PFD_{NEC} is the power flux density computed at various distances, ρ, along the radials, in dBW/m^2-Hz.

ITM transmission loss data and the PFD values at 10 km were combined to calculate PFD values from 10 km out to 50 km. The ITM results used the same ground parameters as NEC, and the same power line height of 12 meters and an assumed receiver antenna height of 42.7 meters.[57] ITM input parameters are detailed in Table 4-5.

Table 4-5: ITM input parameters

Input Variable	Value
Frequency	2-30 MHz in 2 MHz steps
Antenna Heights	Transmitter – 12 m, Receiver – 42.7 m
Siting Criteria	Transmitter – Random, Receiver – Very Careful
Terrain Irregularity Factor, Δh	30 m
Polarization	Horizontal
Relative Permittivity	15
Ground Conductivity	0.005 S/m
Climate	Continental Temperate
Surface Refractivity	301 N-units
Percent Time	50.0%
Percent Location	50.0%
Percent Confidence	50.0%
Mode of Variability	Individual

To determine the PFD values accounting for diffraction losses that come into play at large distances from the power line, the transmission losses beyond 10 km calculated by ITM were scaled relative to the value that ITM computed at 10 km (Equation 4-6). Within 10 km of the power line, the adjusted PFD was the same as the PFD computed using NEC electric field strength directly (Equations 4-5 and 4-7a). Beyond 10 km, the scaled ITM loss values, at each distance, and the PFD computed at 10 km from NEC were used to compute the adjusted PFD (Equation 4-7b).

$$ScaledLoss_{ITM}(\rho) = Loss_{ITM}(\rho) - Loss_{ITM}(10\ km), \quad for\ \rho \geq 10\ km$$

(Equation 4-6)

$$PFD_{Adjusted}(\rho) = PFD_{NEC}(\rho), \quad for\ 0 \leq \rho < 10\ km$$ (Equation 4-7a)

$$PFD_{Adjusted}(\rho) = PFD_{NEC}(10\ km) - ScaledLoss_{ITM}(\rho), \quad for\ \rho \geq 10\ km$$ (Equation 4-7b)

4.3 RESULTS

A summary of the simulation conditions described in Section 4.2 is provided in Table 4-6. The results for computing the receiver noise floor increase along the simulated power line are provided in Section 4.3.1. The results for analyzing the PFD the might be seen by a fixed receiver located at some distance away from the power line are described in Section 4.3.2.

Table 4-6: Simulation conditions

Overhead Power Line Model		
Conductors	3 power conductors, catenary wiring between simulated power pole locations. Multi-grounded neutral conductor. Primarily vertical orientation, switching to horizontal at one location. Four simulated risers connecting to simulated underground load.	
Conductor Material	Copper	
Conductor Thickness	12.6 mm (approx. AWG 4/0)	
Conductor spacing	0.6 m with neutral conductor 1.2 m below	
Model Size	328.2 m in the 'x' direction, 435 m in the 'y' direction	
Height above ground	Power conductors at 12 m with neutral wire at 9.6m	
Coupler location	A coupler was simulated roughly halfway down each of the two main branches and another at the junction of these branches	
Source	1 Volt in series	
Load	7 simulated transformer loads (3 Ω + 5 μH) between power conductors and neutral. Risers had simulated 30 Ω loads between power conductors and ground.	
BPL average duty cycle	55%	
QP-to-RMS conversion	-2 dB	
Ground Conditions		
Conductivity	σ = 0.005 S/m	
Relative permittivity	ε_r = 15	
Simulation Frequencies		
Land Mobile Receiver	2 -30 MHz	
Fixed (*e.g.,* OTH Radar)	2 - 30 MHz	
Receiver Antenna		
Land Mobile	Vertical Whip	
Gain towards power line	0 dBi	
Height	2 m	
Fixed (e.g., OTH Radar)		
Gain towards power line	0 dBi	
Height	42.7 m	
Noise Conditions	Residential, as per Table 4-4	
Land Mobile Simulation	For Noise Floor Increase ((I+N)/N) Analysis	
Victim Receiver Location	Center of simulated roadway	
Power Line Branch	Parallel to x-axis	Parallel to y-axis
Dist. From Power Line	3 m	Ranging from 30 to 48 m

ITM Conditions	For PFD Analysis	
Frequency	2 – 30 MHz	
	Transmitter (Power line)	Receiver (Fixed)
Antenna Heights	12 m	42.7 m
Siting Criteria	Random	Very Careful
Terrain Irregularity Factor, Δh	30 meters	
Polarization	Horizontal	
Relative Permittivity	15	
Ground Conductivity	0.005 S/m	
Climate	Continental Temperate	
Surface Refractivity	301 N-units	
Percent Time	50.0%	
Percent Location	50.0%	
Percent Confidence	50.0%	
Mode of Variability	Individual	

4.3.1 Receiver Noise Floor Increase Along the Power Line

Results were considered from simulations of potential interference to a land mobile receiver on roads next to the simulated power line for all three BPL device injection points across both narrowband and wideband systems, and across frequencies in the 2 to 30 MHz range. The results are presented in terms of the percentage of points along the BPL energized power line that increased the receiver noise floor by various levels.

4.3.1.1 Receiver noise floor increase relative to the injection point

The results shown in Figures 4-4 and 4-5 illustrate the percentage of simulated points along the modeled power line that result in a given level of noise floor increase for all simulation frequencies shown in Table 4-1 for narrowband and wideband BPL signals, respectively. These figures show that the percentage of locations resulting in a given increase in the noise floor varied somewhat by injection point.

The most notable feature of the data is the sharp divergence in the percentage of points for a noise floor increase of 30 dB or more seen by the three modeled injection points. The close proximity of Injection Point 2 to the road and to a modeled transformer load likely accounts for the highest percentages of locations exceeding a 30 dB increase in the noise floor. Injection Point 3 is positioned close to the intersection of three power lines, but at least one utility pole away from nearby transformer loads. This may also have resulted in the increase in the receiver noise floor associated with this point being greater than that of Injection Point 1. Injection Point 1 was located farthest away from the street in this model, and one or more utility poles away from any discontinuities such as transformer loads.

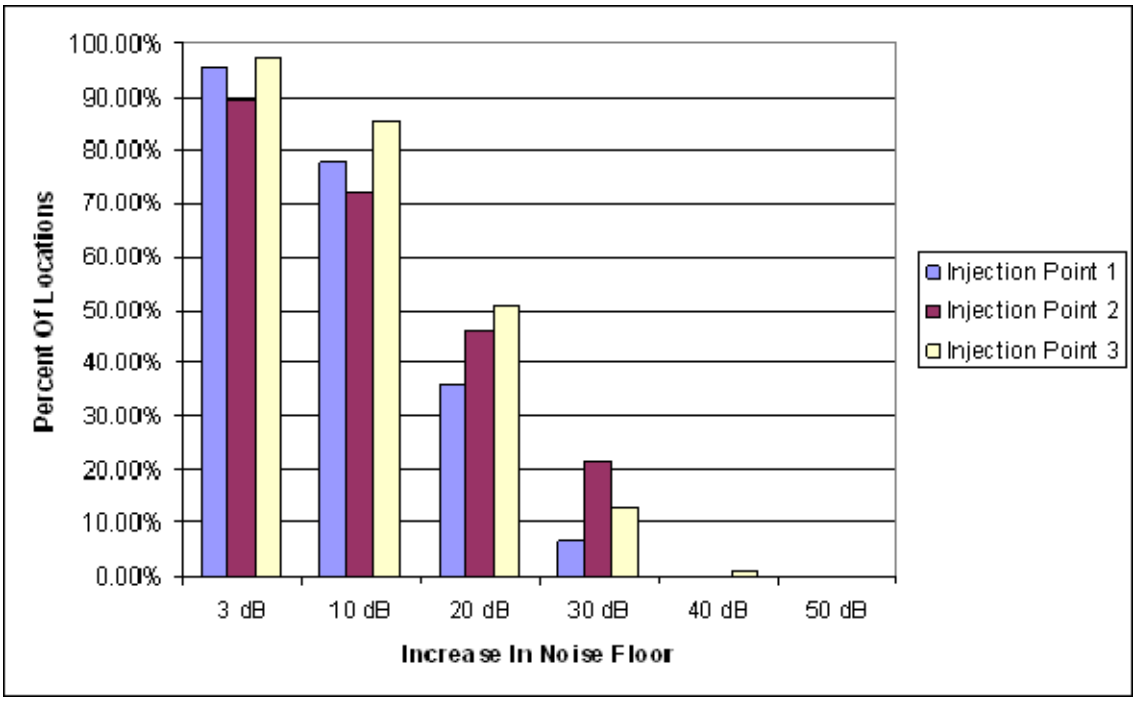

Figure 4-4: Increase in receiver noise floor [(I+N)/N] as a function of the percentage of measurement points around the power line for narrowband BPL signals

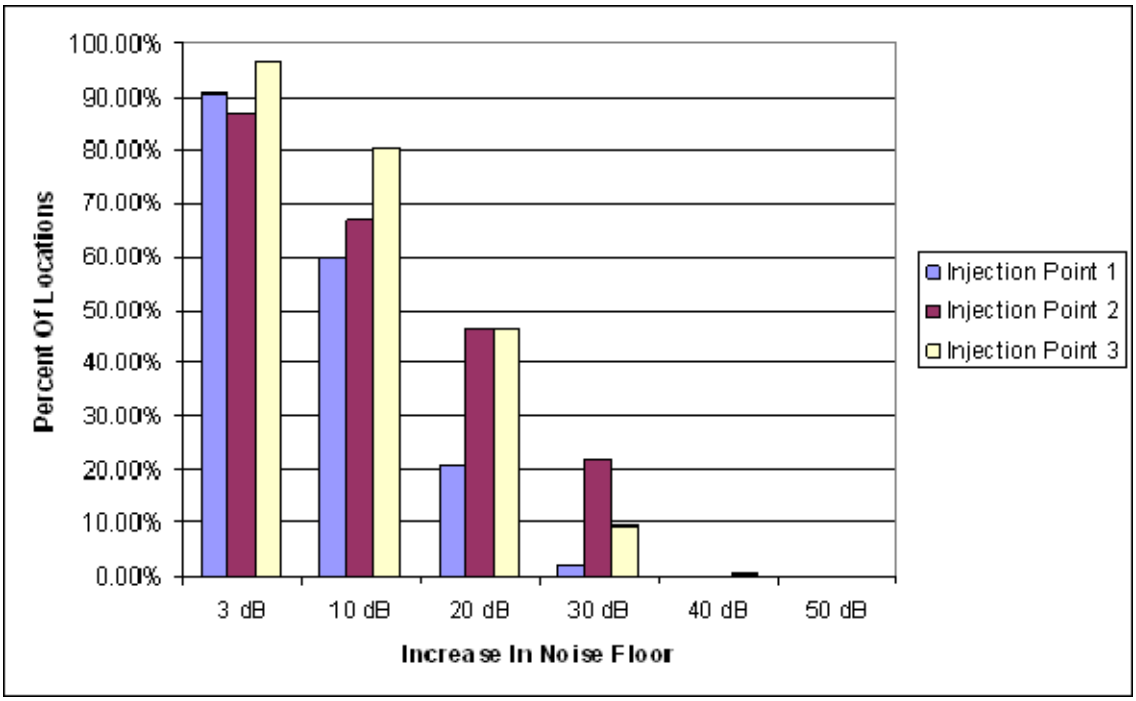

Figure 4-5: Increase in receiver noise floor [(I+N)/N] as a function of the percentage of measurement points around the power line for wideband BPL signals

4.3.1.2 Receiver noise floor increase as a function of frequency

For both narrowband and wideband BPL signals, variation was noted in the calculated results over frequency. Table 4-6 shows the results for narrowband signals and Table 4-7 shows results for wideband signals based on simulations for Injection Point 3.

Table 4-6: Percentage of simulated points along the power line at which the receiver noise floor was increased by at least the specified amount for narrowband BPL signals

Frequency Band (MHz)	Noise Floor Increase (dB)					
	3	10	20	30	40	50
2-6	95.22%	67.97%	34.29%	9.50%	0.00%	0.00%
6-10	95.83%	80.59%	38.81%	4.78%	0.00%	0.00%
10-14	97.39%	82.30%	47.41%	12.57%	0.00%	0.00%
14-18	98.94%	87.53%	61.04%	20.97%	2.46%	0.00%
18-22	98.94%	92.86%	63.90%	20.76%	1.56%	0.00%
22-26	98.49%	90.60%	49.17%	5.68%	0.00%	0.00%
26-30	99.20%	95.22%	60.78%	14.98%	0.00%	0.00%

Table 4-7: Percentage of simulated points along the power line at which the receiver noise floor was increased by at least the specified amount for wideband BPL signals

Mid-band Frequency (MHz)	Noise Floor Increase (dB)					
	3	10	20	30	40	50
4	93.51%	56.71%	22.02%	1.81%	0.00%	0.00%
6	88.99%	60.94%	28.66%	0.00%	0.00%	0.00%
8	99.40%	87.03%	43.59%	3.62%	0.00%	0.00%
10	95.78%	81.75%	37.71%	3.17%	0.00%	0.00%
12	96.08%	79.49%	50.38%	7.69%	0.00%	0.00%
14	98.19%	78.58%	47.96%	14.78%	0.00%	0.00%
16	98.04%	82.20%	42.53%	0.60%	0.00%	0.00%
18	99.70%	97.89%	82.81%	39.06%	4.68%	0.00%
20	98.64%	92.91%	61.24%	11.46%	0.00%	0.00%
22	98.34%	86.73%	46.30%	10.86%	0.00%	0.00%

4.3.2 Power Flux Density Away from the Power Line

The away-from-the-line analysis computed the PFD seen by a fixed receiver, such as an OTH radar receiver, as a function of distance of the receiver from the modeled Access BPL system. The PFD as a function of distance was determined for the three modeled BPL injection points and frequency bands for narrowband and wideband BPL signals. In considering these results, NTIA looked at median values for both narrowband and wideband BPL signals across radials leading away from the power line model and across the 2 to 30 MHz frequency band.

Figures 4-6 and 4-7 depict median PFD versus distance from the origin for all simulated in-band frequencies for the three BPL injection points described in Section

4.2.2. Variation in PFD as a function of horizontal distance for the different injection points on the structure was very small and did not exceed 3 dB at any given distance from the power line model.

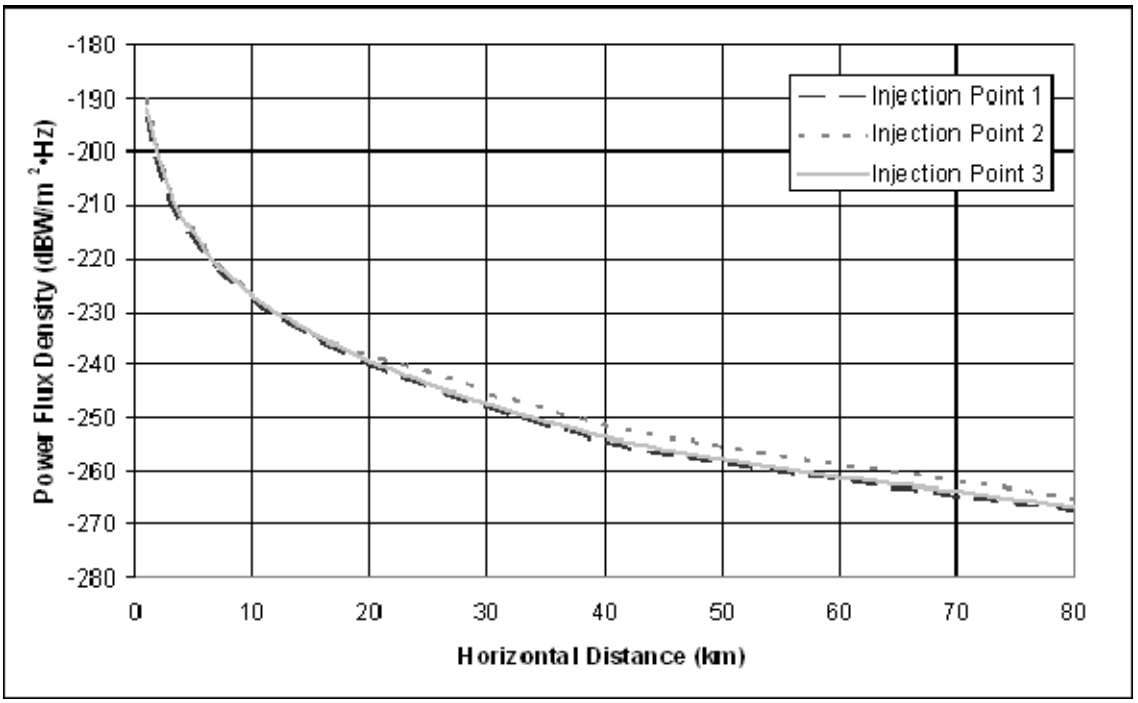

Figure 4-6: Power Flux Density as a function of distance from the origin for narrowband BPL signals across all simulated in-band frequencies

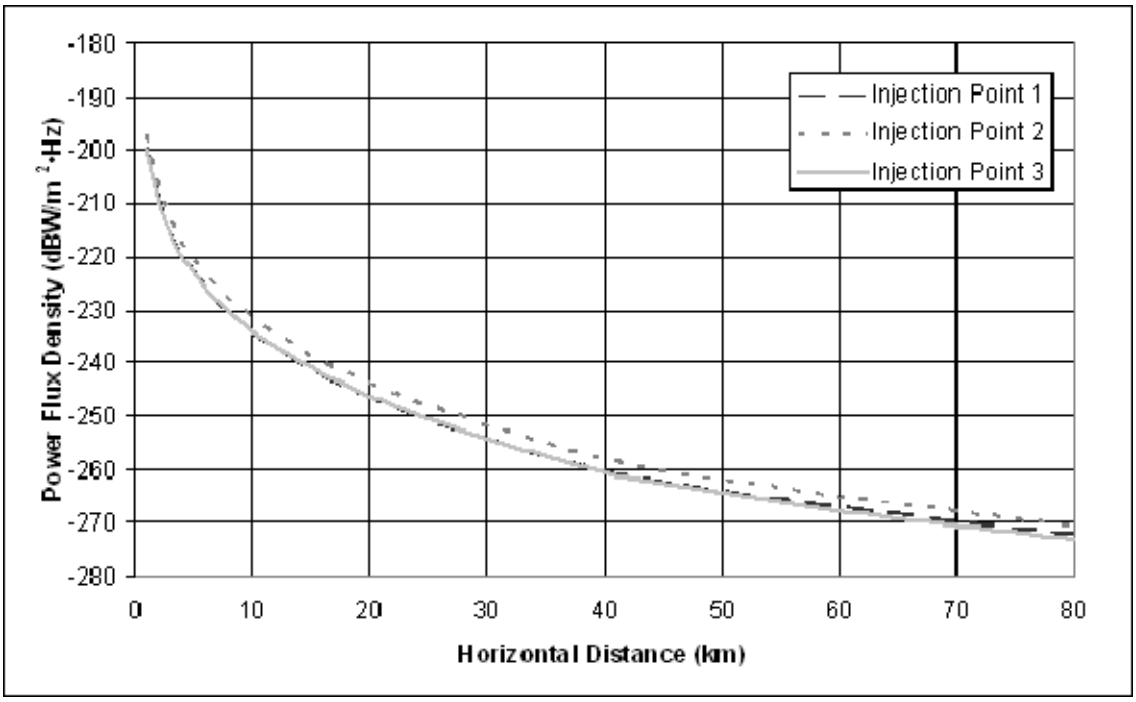

Figure 4-7: Power Flux Density as a function of distance from the origin for wideband BPL signals across all simulated in-band frequencies

When considering frequency as a factor, the median (with respect to azimuth) PFD results from Injection Point 3 as a function of distance take on more variation. As shown in Figures 4-8 and 4-9 for the narrowband and wideband BPL signals, respectively, the maximum variation as a function of frequency was approximately 13 dB at 1 km distance for narrowband BPL signals and nearly 15 dB at 4 km distance for wideband BPL signals.

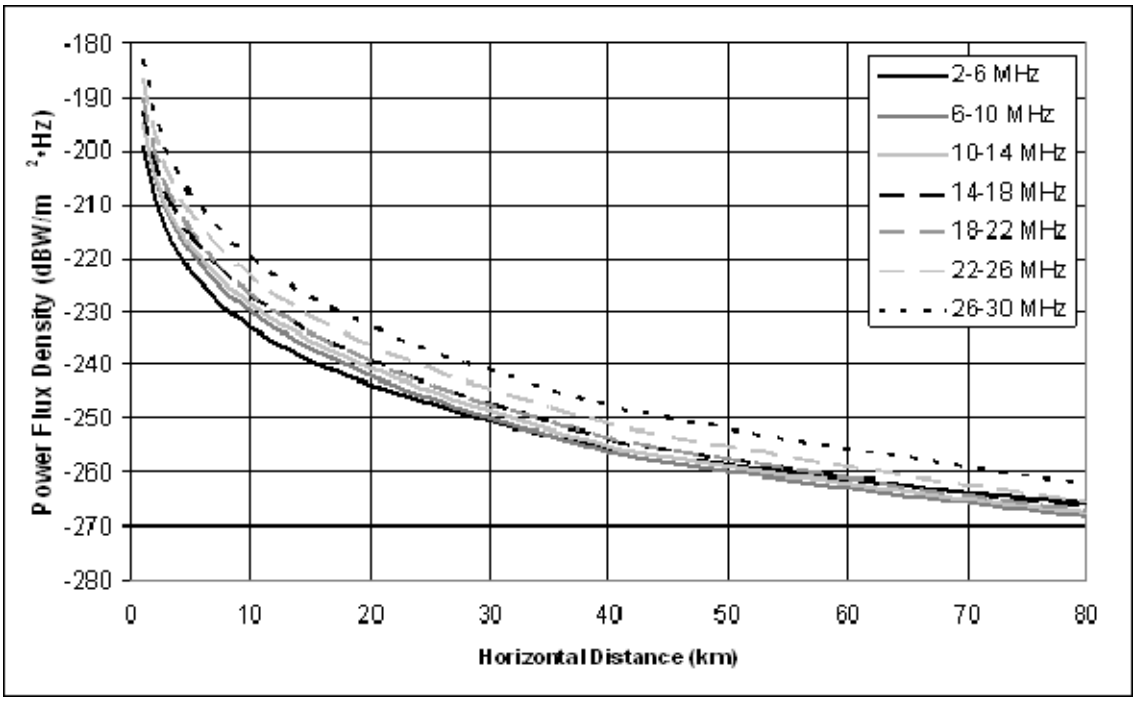

Figure 4-8: Power Flux Density as a function of distance from Injection Point 3 for narrowband BPL signals, organized by frequency band

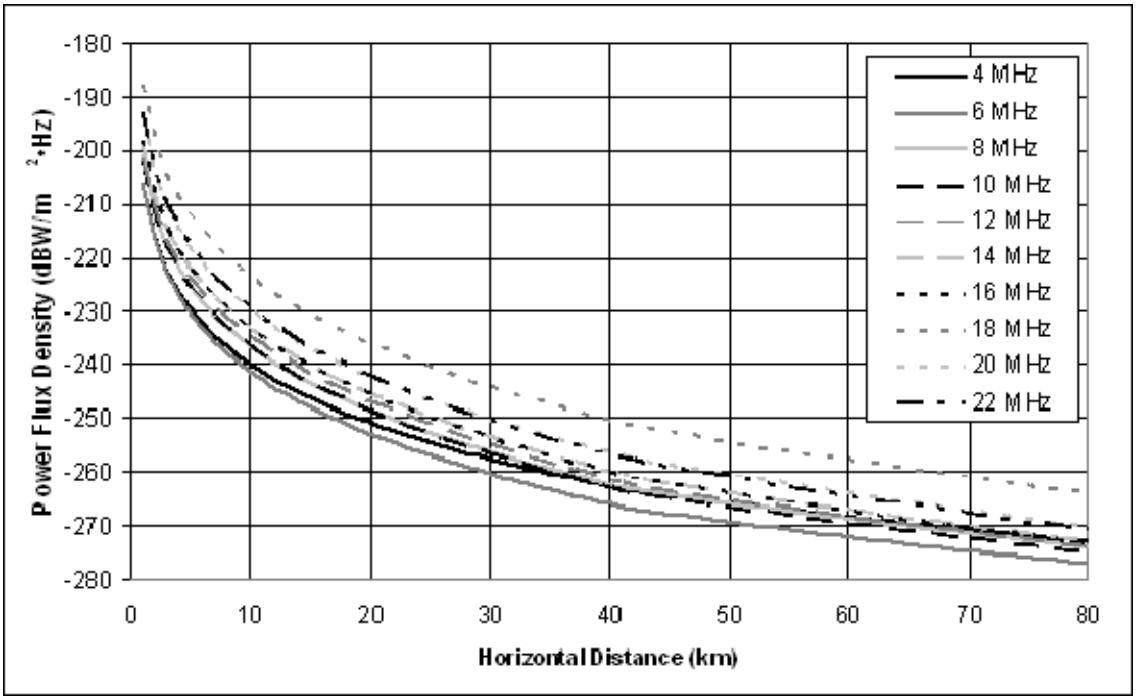

Figure 4-9: Power Flux Density as a function of distance from Injection Point 3 for wideband BPL signals, organized by frequency

For the narrowband BPL signals shown in Figure 4-8, the PFD level at any given distance tends to increase as the frequency band increases. This trend results primarily

from increasing radiated power as frequency increases. In other words, the total radiated power of this model tends to increase as frequency increases, while still meeting the Part 15 electric field strength limit as measured using the Commission's measurement guidelines. For wideband BPL signals, where Part 15 scaling relies on the measurement locations associated with the midband frequency (Table 4-2), the estimate of electric field strength for some individual frequencies may be somewhat less accurate. This may be observed in the variability of PFD levels for each frequency band shown in Figure 4-9, where the calculated PFD levels do not consistently increase with frequency.

4.4 SUMMARY

The NTIA case study illustrates application of the Commission's Part 15 rules and measurement guidelines for Access BPL systems. NTIA analyzed the potential impact on mobile radiocommunication systems close to an overhead BPL-energized power line emitting RF energy at the Part 15 limit, as well as to fixed radiocommunication systems, (such as OTH radars) at great distances from the line. While previous analyses made use of simple power line models, this case study employed an elaborate power line model that included a variety of features found in an actual MV power distribution system carrying BPL signals.

The results of this analysis are comparable to those found in NTIA's earlier investigations, and indicate that the Part 15 measurement procedures described in the BPL Report and Order appear to estimate adequately the electric field strength levels around the power line near ground level.[58]